ELSEVIER

Advances in Engineering Software 37 (2006) 184–194

ADVANCES IN ENGINEERING SOFTWARE

www.elsevier.com/locate/advengsoft

Neural network with multi-trend simulating transfer function for forecasting typhoon wave

H.K. Chang, W.A. Chien*

Department of Civil Enginering, National Chiao-Tung University, Hsinchu 300, Taiwan, ROC

Received 2 September 2004; received in revised form 5 February 2005; accepted 29 April 2005
Available online 24 August 2005

Abstract

This study develops an NN typhoon wave model to accurately and efficiently calculate wave heights at a point of interest. Multi-trend simulating transfer functions were first introduced to exemplify the relationship between wave heights and each conceivable input factor by regressive fitting. The proposed NN–MT model can accurately forecast wave peak with an error of less 1.2 m and with time delay within 3 h and can be extended to cover the station besides the original station of interest.
© 2005 Elsevier Ltd. All rights reserved.

Keywords: Neural network wave model; Trend simulation; Transfer function; Peak wave height

1. Introduction

On average, 3.5 typhoons pass near or over Taiwan annually. Strong typhoon winds blow over the sea and produce large waves with enough energy to influence marine structures and erode beaches. Consequently, some researchers in Taiwan have produced models of wind and waves to forecast typhoon wind and wave patterns. Both empirical regression and numerical models can estimate the wave heights and periods of typhoon waves. Parametric wave expressions offer an easy and quick calculation of typhoon wave heights and periods, e.g. Bretschneider [2]. The parametric expressions are usually confined to local waters and cannot be extended to a large area. Large areas prefer numerical models based on the conservation of energy to calculate the wave heights and periods, including Chen and Wang [5], SWAMP [22], WAM [25], Young [26], SWAN (Booij et al. [1]) and WW_3 (Tolman [24]), Niwa and Hibiya [20].

Correct wind speeds in spatial grids and time domains are needed as energy input sources in the numerical models. However, in practice too few measurements are available to support the spatial minimum requirement in computation. Modern information on the dynamical processes of generation, interaction and decay of ocean waves accumulated over the last 40 years. The renowned Phillips–Miles theory was reviewed and supplemented by authors (Kismann [15]; Krasitskii [17]; Riley et al. [21]; Chalikov and Makin [3]; Komen et al. [16]), although the Phillips–Miles theory still predicts energy transfer rates that are smaller than measured values. Much computational time is desired to run the numerical models owing to repeated iteration in many grids for a large area. Due to less wind data measured, uncertain mechanisms of air–sea interaction and computation time, numerical models cannot yield to simultaneously have quick and accurate calculations for typhoon wave heights for some interesting point, particularly during typhoon periods.

The artificial neural network (NN) is a powerful new tool because of its high functioning with fast computation and a considerable memory to solve the problems concerning extremely non-linear interactions and complex effective variables. Accordingly, NN has newly been implemented widely in different areas. For example, Hajime et al. [9] employed NN to explore the stability of rubble-mound breakwaters. Johnson and Lin [14] used a back-propagation network, which is one type of NN, to determine the path of the typhoon. Assessment of their findings with those obtained using an ARIMA model displays that their NN model has a better forecasting capability than the ARIMA model. Tsai and Lee [23] developed an NN model to

* Corresponding author. Tel.: +886 3 571 2121; fax: +886 3 572 6111.

0965-9978/$ - see front matter © 2005 Elsevier Ltd. All rights reserved.
doi:10.1016/j.advengsoft.2005.05.001

forecast the levels of diurnal and semi-diurnal tides. Lee and Liu [18] utilized NN associated with satellite images, in tropical cyclone pattern identification to determine the paths of the cyclones. Hiraoka et al. [11] developed an NN model, based a two-rule fuzzy theory, to calculate the location of the typhoon. Deo and Naidu [6] used NN to establish a real-time wind model. Deo et al. [7] developed an NN Wind–Wave model.

If wave data from some observation stations and corresponding typhoon data are available, then NN can be used to set up interconnections between waves and winds, by taking advantage of its ability to learn and adapt. Chang et al. [4] proposed two NN typhoon wave models that are made by linking the typhoon wind speeds at the interesting point and a sequence of typhoon's positions to the wave heights observed. They are then tested to accurately calculate wave heights and periods when the track of a typhoon is alike to those in the learning stage. These two NN models proposed by Chang et al. [4] have poor prediction to the wave heights for special typhoon tracks that are far away from those used in the learning stage, because insufficient data are collected in the learning stage to cover possible typhoon tracks.

Based on the understandings of the former NN model, our results indicate that the position of an interesting point in a typhoon is a significant factor that was not involved in the former models. Additionally, several usually anticipated transfer functions, e.g. Satlin, between wave heights and each input parameter are not appropriate in the whole domain. Therefore, this study revises the former NN models by using regressive multi-trend transfer functions that can moderately and confidently describe the trend of wave heights and each input parameter. The purpose of this work is to develop an NN typhoon wave model for accurately and quickly calculating the wave heights at a point of interest.

2. Input parameters

Polar coordinates with the origin at the center of the typhoon are used to demonstrate the relative position between the point of interest and the center of the typhoon. The polar coordinates (r, θ_1), shown in Fig. 1, refer the radial distance and azimuth between the point of interest and the center of the typhoon.

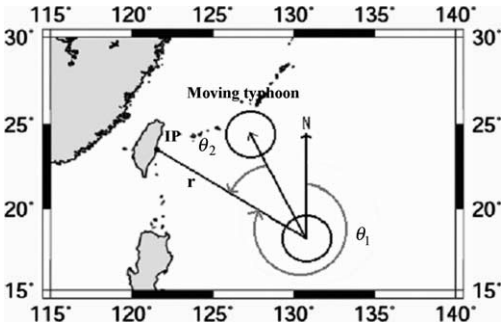

Fig. 1. Sketch definition of input parameters.

Generally most typhoons initially form within one warm, humid air between 10 and 25° latitude in both hemispheres, and then move westward and pole-ward at a speed of 5–40 km/h. Strong wind inside a typhoon is clearly important to wind wave development. Whether the energy of wind waves rises or decreases mostly depends on the energy input from the winds. Thus, the key of calculating the typhoon waves is accurately to evaluate the local wind speeds associated with a typhoon. The local wind speed can be measured at an observation station. However, wind stations are too few to yield adequate data because of costly construction and instrument maintenance. Some parametric typhoon models have already been presented to explicate explicitly the local wind speed at any point inside a typhoon. These include the Rankine-Vortex model, the SLOSH (Sea, Lake and Overland Surge from Hurricane) wind model and the Holland's [12] model, which are applicable.

The typhoon wind field is extremely complex and irregular that an accurate distribution of the wind in a typhoon field is required to permit sufficiently accurate information to be input to a wave model. Holland's wind model [12] is adopted here because it fairly describes a typhoon's winds. The wind speed at a distance r from the center of the typhoon is

$$V(r) = \left[\frac{B\Delta p_c}{\rho}\left(\frac{R_{max}}{r}\right)^B \exp\left[-\left(\frac{R_{max}}{r}\right)^B\right] + \frac{r^2C^2}{4}\right]^{0.5} - \frac{rC}{2} \quad (1)$$

where C is the Coriolis parameter. The maximum wind speeds in a typhoon are obtained by specifying $r = R_{max}$ in Eq. (1). Harper and Holland [10] suggested a value of B of

$$B = 2 - \frac{p_c - 900}{160}, \quad 1.0 < B < 2.5 \quad (2)$$

The local wind speed 10 m above mean sea level is proportional to $V(r)$ and can be written,

$$V_{10} = K_m V(r) \quad (3)$$

where $K_m = 0.7$, as also recommended by Harper and Holland [10]. If a typhoon moves at speed V_f, then the modified local wind speed, as given by Jelesnianski [13], can be expressed as:

$$V(r) = \frac{R_{max} r}{R_{max}^2 + r^2} V_f \quad (4)$$

When the pressure depression (Δp_c) at the center of a typhoon, and the distance between the point of maximum wind speed and the typhoon's center are given, the local wind speed 10 m above sea level, V_{10}, and V_{max} can be determined from Eqs. (1)–(4), at any position inside the typhoon. According to the Holland typhoon wind model, the parameters of Δp, V_{max}, V_f, V_{10} and R_{max} are related.

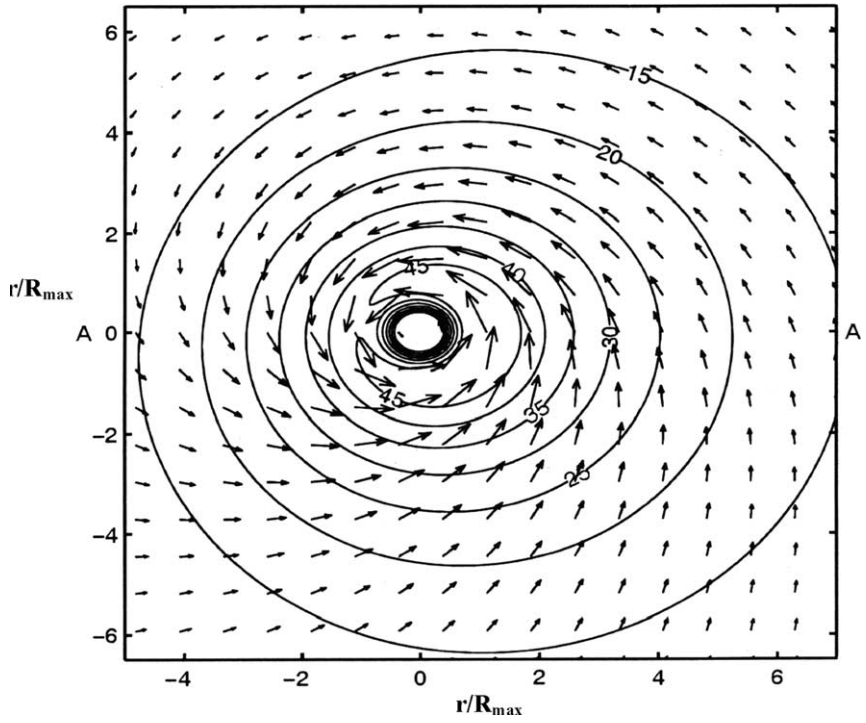

Fig. 2. The computed wind velocity field in a typhoon with $\Delta p = 930$ mb and $V_f = 5.0$ m/s by using the Holland model.

Fig. 2 demonstrates the wind velocity distribution of a moving typhoon with $\Delta p = 930$ mb and $V_f = 5.0$ m/s computed by the Holland model. The iso-speed contours in Fig. 2 are in an oval-like form signifying that the wind velocity is not isotropic. The wind speed in the right half of the semi-circle is larger than that in the left semi-circle at the same radial distance. The wind speed distribution in the right semi-circle differs from that in the left semi-circle. Accordingly, the angle of an interesting point in a typhoon becomes an essential indicator to describe the wave heights. Let θ_2 be the angle of an interesting point in a typhoon between the typhoon moving direction and the radial direction from the typhoon's eye to that point. The value θ_2 counts counterclockwise. Thus, when the interesting point is on the way of the typhoon moving direction, θ_2 is zero. When the interesting point is on the left semi-circle of a typhoon θ_2 is less than π. The interesting point is on the right half of semi-circle of a typhoon showing $\pi < \theta_2 < 2\pi$.

The moving track, speed and scale of a typhoon dominantly and together influence the waves in or near the typhoon. The wave at time t accumulatively consists of a sequential superposition of waves that may propagate at a different speed but simultaneously reach the interesting point at time t. Thus, the wave height can be written in a sum of energy source function in a sequential time as follows

$$H_s(t) = \sum_{m=0}^{n} a_m f(V_{10},\ r,\ \theta_1,\ \theta_2;\ t - m\Delta t) \tag{5}$$

where Δt is the sampling rate and a_m is the coefficient. Eq. (5) reveals that the wave height of an interesting point at time t is an output resulting from accumulative action of an n-hour sequence of wind parameters, V_{10}, r, θ_1 and θ_2 where V_{10}, r, and θ_1 are three dominant factors of a typhoon affecting typhoon waves shown by Chang et al. [4]. The angle θ_2 is a corrector factor indicating the wave distribution in a typhoon. If amount of well distributed input data are absent, the extra input data in the NN model will make worse prediction accuracy. Avoiding disadvantages of less information or a bias distribution of input data we first relate the wave heights and each input data to provide a good relationship in the model and to promote the model prediction capacity. For a detailed description of θ_2, equal quarter around a circle is divided to have its distribution function in Section 3.

3. Construction of NN–MT model

3.1. Normalization of input data

The value of input data should be normalized in a range of 0–1 to match the requirement of transfer functions used in an NN model. The wave data are observed by the waverider that is located at a depth of 25 m. Historically the maximum wave height observed is 8.4 m. Wave height of 12 m, that is around 50% more than the maximum wave height observed, is allowed as the basic quantity to normalize all wave heights observed.

Such the maximum wave height observed at the Hua-Lien harbor was generated by an wind speed of $V_{10} =$ 25 m/s. A strong typhoon in typhoon scales is identified to

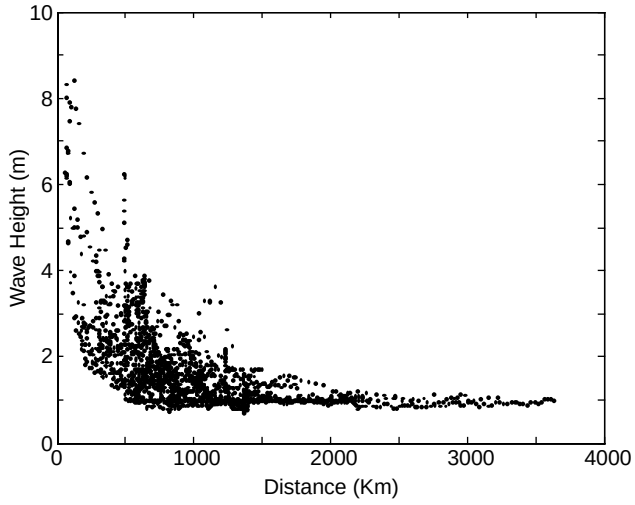

Fig. 3. Data plots of the wave heights observed vs. the distance between the typhoon and the observation station.

have a maximum wind speed range of 32.7–50.9 m/s. Taking an average of upper and lower speed bounds of a strong typhoon yields 41.8 m/s. Substituting the mean value to Eq. (3) leads to $V_{10} \approx 29.3$ m/s. Thus 30 m/s is acceptable as a basic quantity for the wind speed.

The wave height observed relating to the distance between the typhoon and observation station is illustrated in Fig. 3. Generally, a typhoon with strong wind speeds extends to 200–500 km. From Fig. 3, when the observation point is distant from a typhoon by 1500 km the wave heights differ somewhat. Accordingly, the wind speed of a typhoon affecting waves is understood to be limited in a circle with a semi-diameter of 1500 km. The distance between an interest observation and typhoon eye used in this model is then normalized by 1500 km. Here, 2π is used to be an angular basic quantity to make both θ_1 and θ_2 in a range of 0–1. These four normalized parameters are denoted by $\bar{V}_{10}, \bar{r}, \bar{\theta}_1,$ and $\bar{\theta}_2$, respectively.

3.2. Multi-trend transfer functions

The transfer function in an NN model is to relate the inputs to the outputs. A valid transfer function that can certify the model for most cases. Four multi-trend transfer functions for each input parameter are introduced by using statistical regression. Therefore, the proposed NN model is referred to here as a neural network typhoon wave model with multi-trend transfer functions, abbreviated by NN–MT. If the average regression is taken to fit the relationships between each input and the output, the weight matrix obtained in NN maybe have some weights enlarged and some weights disregarded so that some input parameters fail to reflect the possibly fair relationships between these inputs and the output. The transfer functions proposed are conventionally adopted in NN and approximately fit the relationship between each input parameter and the output.

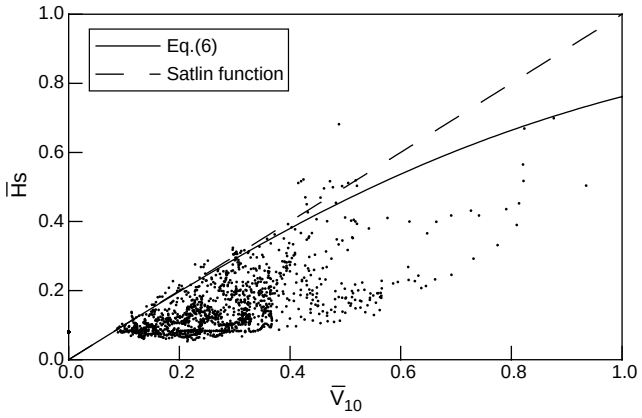

Fig. 4. Data plots and the functional relationships between the normalized wave heights and wind speeds.

These transfer functions thus address trend fitting. Here, four transfer functions for four input parameters are introduced as follows.

3.2.1. Transfer function for $\bar{V}_{10}$

Fig. 4 reveals that wave growth positively and exponentially depends on wind speeds and in the initial growth, the wave heights more rapidly increase than those in high wind speeds. The trend performance between the waves and wind speeds can be expressed by the transfer function for wind speed, $f_{\bar{V}_{10}}$, as follows

$$f_{\bar{V}_{10}} = \frac{2}{(1 + e^{(-2\times\bar{V}_{10})})} - 1 \tag{6}$$

in which the form is one of the typical transfer functions, called hyperbolic tangent sigmoid transfer function, in Matlab software and is appropriate for describing how wave height and wind speed are related. The dashed line in Fig. 5 shows the Satlin transfer function, which is also an available transfer function in the Matlab software, used in the NN2 of Chang et al. [4]. When $\bar{V}_{10} = 0$, Eq. (6) gives $f_{\bar{V}_{10}} = 0$. When $\bar{V}_{10} = 1$, $f_{\bar{V}_{10}} = 0.762$ is obtained by Eq. (6). Thus, $f_{\bar{V}_{10}}$ varies in a range of 0–0.762. For a small $\bar{V}_{10}$, the Satlin transfer function and Eq. (6) provides an equivalent prediction to the wave heights. However, Eq. (6) more accurately predicts the wave heights than the Satlin transfer function does for a large $\bar{V}_{10}$. Eq. (6) displays a similar trend to the wave heights observed shown in Fig. 4.

3.2.2. Transfer function for $\bar{r}$

The typhoon wind model states that the wind speed increases with the distance from the center until the maximum wind speed and then exponentially decreases with distance from the maximum wind speed to the outer part of the typhoon. Fig. 5 illustrates the relationship between the wave height and the distance of the interest point from the typhoon eye. Fig. 5 describes that the wave height decreases as the distance from typhoon eye increases. This trend can be fitted by symmetric Gaussian functions in

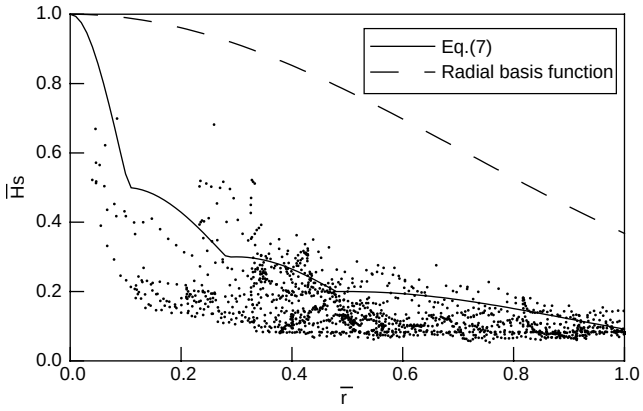

Fig. 5. Data plots and the functional relationship between the wave height and the distance of the interest point from typhoon eye and the proposed transfer functions.

four pieces. The symmetric Gaussian function that is also a typical transfer function in Matlab software is examined to give $f\bar{r}$

$$f\bar{r} = \mathrm{Max}(f_{\bar{r}_1},\ 0.5f_{\bar{r}_2},\ 0.3f_{\bar{r}_3},\ 0.2f_{\bar{r}_4}) \tag{7a}$$

where

$$f_{\bar{r}_i} = \mathrm{e}^{-(\bar{r}-c)^2/2\sigma^2}, \qquad i = 1,\ 2,\ 3,\ 4 \tag{7b}$$

Two parameters $(c,\ \sigma)$ in the Gaussian function are (0, 0.05) for f_{r_1}; (0.15, 0.1) for f_{r_2}; (0.2, 0.3) for f_{r_3}; and (0.4, 0.5) for f_{r_4}. The radial basis transfer function used in the NN2 of Chang et al. [4] and Eq. (7) are drawn in the Fig. 5 by a dashed line and a solid line, respectively. The suggested transfer function for $\bar{r}$ is much closer to the observed data than the radial basis transfer function.

3.2.3. Transfer function for $\bar{\theta}_1$

Expressing the relationship between a typhoon position and an observation point in polar coordinates rather than Cartesian coordinates is convenient. Wave propagation is independent of θ_1 so that a linear transfer function is valid for $\bar{\theta}_1$ and can be written as

$$f_{\bar{\theta}_1} = \bar{\theta}_1, \qquad 0 \le \bar{\theta}_1 \le 1 \tag{8}$$

3.2.4. Transfer function for $\bar{\theta}_2$

According to Fig. 2 the wind velocity distribution in a typhoon stated in Section 2, wind speed distribution in a typhoon is separated into four quarters shown in Fig. 6. The transfer function for $\bar{\theta}_2$ is also selected in the form of Gaussian function with different mean and variance for each quarter. Gaussian function can efficiently separate four quarters and represent the change of wind directions in each quarter. When the observation point is located at the conjunction of two neighboring parts, the effect of $\bar{\theta}_2$ at one part on waves differs from that of the other part. Therefore, the transfer function for $\bar{\theta}_2$ must differentiate the effect of one part from that of the other. Fig. 2 indicates that

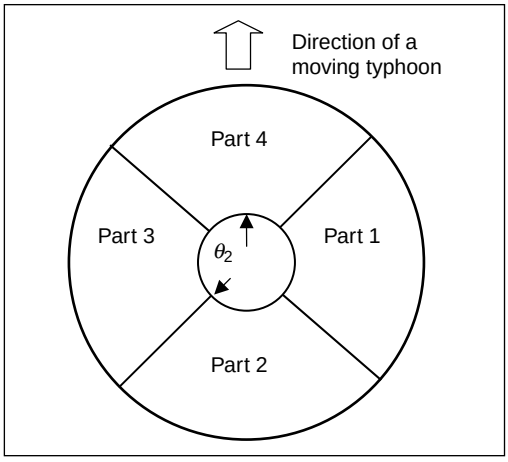

Fig. 6. Schematic diagram of four quarters of the wind speed distribution in a typhoon.

the angle $\bar{\theta}_2$ also varies with the distance between the observation and the typhoon center. Thus, transfer function for $\bar{\theta}_2$ is defined as

$$f_{\bar{\theta}_2} = \mathrm{Max}(\mathrm{e}^{-((\bar{\theta}_2-c_1)^2/2\sigma_1^2)},\ \mathrm{e}^{-((\bar{\theta}_2-c_2)^2/2\sigma_2^2)})f\bar{r}, \qquad c_1 > c_2 \qquad f_{\bar{\theta}_2} = f\bar{r}, \quad c_1 > c_2 \tag{9}$$

where the coefficients $(c_1, \sigma_1, c_2, \sigma_2)$ are given in each quarter as follows: (0.66, 0.05, 0.84, 0.05) for the region $f_{\bar{\theta}_{21}}$; (0.41, 0.05, 0.59, 0.05) for the region $f_{\bar{\theta}_{22}}$; (0.16, 0.05, 0.34, 0.05) for the region $f_{\bar{\theta}_{23}}$; (0.91, 0.05, 1.0, 0.05) or (0.0, 0.05, 0.09, 0.05) for the region $f_{\bar{\theta}_{24}}$. The final coefficient group depends on which one gives larger $f_{\bar{\theta}_{24}}$ than does the other one.

The trend transfer function for $\bar{\theta}_2$ in the first quarter illustrated in Fig. 7 is taken an example. The shapes of four transfer functions are all in the form of Gaussian distribution with a different mean value that indicates the mean angle of $\bar{\theta}_2$ in each quarter. For example, the first quarter is located on the right semi-circle that has a mean direction pointing to the right. Accordingly θ_2 is 270° for this mean direction implying that $\bar{\theta}_2 = 0.75$ shown in Fig. 7.

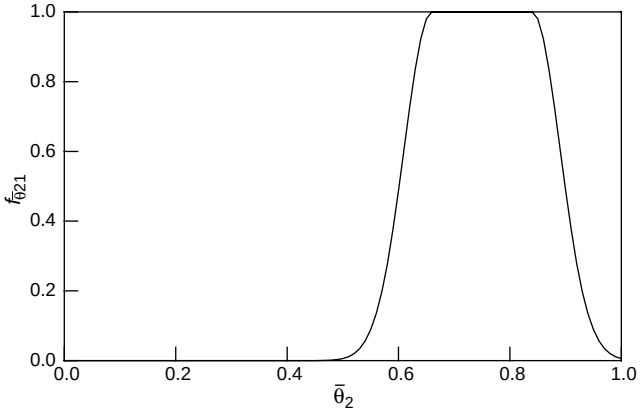

Fig. 7. The transfer function for the first quarter $f_{\bar{\theta}_{21}}$ when $f_r = 1$.

When the number of input data is small or the data are abnormally distributed, an NN model is hard to accurately simulate wave heights. From wind theory or empirical understanding, wind speed in the right semi-circle exceeds that in the left semi-circle and both semi-circles have different distributions. Reasonable expressions of wind distribution from theory or empirical understanding can be given to improve the simulating capacity of an NN model due to less data or abnormal distribution of $\bar{\theta}_2$. This study investigates how $\bar{\theta}_2$ affects wave heights and proposes two models. One model is named by NN3 to use an accessible Satlin transfer function Matlab software and the other model, NN–MT, employs the Gaussian function distributed in four quarters of a circle.

3.3. Algorithm of NN–MT typhoon wave model

The present NN–MT model mainly consists of two stages, shown in Fig. 8. The first stage attempts to enhance the functional relationships between the normalized input data and the normalized wave heights by using the corresponding trend transfer functions. The operation procedure initially calculates the values of four input parameters, V_{10}, r, θ_1, and θ_2, at the interesting point. Second, to normalize these four different input data types by using their corresponding basic quantities stated in Section 3.1 and then to add them into trend transfer functions, Eqs. (8)–(11), yields seven kinds of normalized data, $f_{\bar{V}_{10}}, f_{\bar{r}}, f_{\bar{\theta}_1}, f_{\bar{\theta}_{21}}, f_{\bar{\theta}_{22}}, f_{\bar{\theta}_{23}}$, and $f_{\bar{\theta}_{24}}$. The second stage aims to identify the time delay effect of winds on wave heights. This stage uses two hidden layers to obtain the optimal weight matrix and bias matrix by minimizing the error square of the outputs computed and the normalized wave heights measured.

Back-propagation neural network (BPNN) is selected to implement the typhoon wave model owing to its highly effective simulation for both linear and non-linear problems. The elaborate introduction to the related theories and computational algorithms of BPNN can refer to Eberhar and Dobbins [8] and various textbooks. Lippman [19] addressed that a 2-hidden-layer NN is sufficient to simulate a problem that includes a highly non-linear interaction or discontinuity.

Typically, an applicable BPNN model is validated in a learning stage and a verification stage. When the errors of each interaction in both the learning stage and the verification stage are simultaneously decreasing, the model continues to learn. Conversely, whenever the error magnifies, the model stops learning. When the simulation error reaches an assigned minimum, the optimal weight and bias matrices have been set. To simulate typhoon waves accurately, the model must pass the verification stage. If an NN has one hidden layer the output can be expressed by a function of the inputs as follows

$$O_{P\times 1} = f_1(W_{S\times R} I_{R\times 1} + b_{S\times 1}) \tag{10}$$

where $O_{P\times 1}$ denotes the output matrix of P vectors; $f(W, I, b)$ represents the transfer function; $I_{R\times 1}$ is the input matrix of R vectors and $W_{S\times R}$ and $b_{S\times 1}$ are the weight matrix and the bias matrix, respectively, of an NN with S neurons. Eq. (10) reveals that each input, multiplied by a weight and then altered by an added bias, can be connected to an output through a transfer function.

The output in the proposed NN model with two hidden layers is the significant wave height and can be written

$$H_s = f_2(W_{S2\times S1} \times f_1(W_{S1\times(R\times n)}[I_{R\times 1}]_{n\times 1} + b_{S1\times 1}) + b_{S2\times 1}) \tag{11}$$

where $I = [f_{\bar{V}_{10}}, f_{\bar{r}}, f_{\bar{\theta}_1}, f_{\bar{\theta}_{21}}, f_{\bar{\theta}_{22}}, f_{\bar{\theta}_{23}}, f_{\bar{\theta}_{24}}]^T$, n is the time lag.

Generally, the waves propagating away from a typhoon have a wave period of 10–14 s. A wave in deep water with a period of 12 s propagating in a speed of 18.72 m/s takes 22.25 h to go a distance of 1500 km. Thus, a 24-h time lag is considered in the present model. To aid the computation time, each input is simultaneously selected from time series for every 4 h instead of every hour, i.e. at the time t, $t-4$, $t-8$, …, $t-24$. Thus, the total number of inputs is 49. The neurons in the first hidden layer are 80, and 40 neurons in

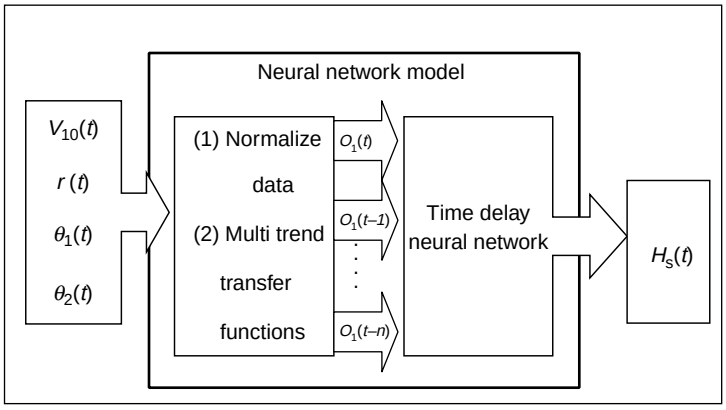

Fig. 8. The construction of the present NN model.

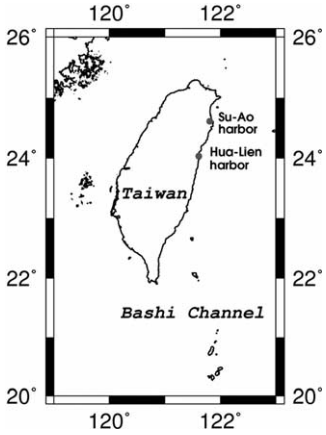

Fig. 9. Locations of the Hua-Lien and Su-Ao harbors.

the second hidden layer. The proposed NN–MT model is thus designated by (49-80-40-1).

4. Model calibration and verification

4.1. Model calibration

Typhoon wave data beyond the Hua-Lien harbor, on the eastern coast of Taiwan, are used to establish the present NN models, which are extended to the Su-Ao harbor that neighbors the Hua-Lien harbor at a distance of about 70 km. Both harbors are on the eastern coast of Taiwan, as depicted in Fig. 9.

The Center for Harbor and Marine Technology, Institute of Transportation, Ministry of Transportation and Communications, Taiwan, collected the wave data, using an SP-2200 wave and tide gauge, developed by Woods Hole Instrument Systems, positioned 0.5 m above the sea bed at a depth of approximately 25 m. The sampling rate was set to 2.56 Hz, and the sampling period was 20 min in each hour. Each data set includes 3072 pieces of data.

The typhoon's position and scale data were obtained from the Central Weather Bureau of Taiwan (CWB, whose website is http://www.cwb.gov.tw/), the Joint Typhoon Warning Center (JTWC, whose website is http://manati.wwb.noaa.gov/) and UNISYS WEATHER (whose website is http://weather.unisys.com/). The name of the typhoon given by JTWC and Greenwich Mean Time (GMT) were used. The typhoon data were sampled every 6 h. Third-order Lagrangian interpolation to transform 6 h of typhoon data into 1-h of data was applied to match the 1-h wave data. Fig. 10 plots the paths of these nine typhoons.

In the learning stage, all data collected from nine typhoons are in a sequence. The total number of data is 2500. The authors add an extra 24-h data in the beginning and at the end of each typhoon to have the model to clearly identify each typhoon separated. The added wave heights are the measured mean significant wave heights caused by monsoons. The distance between an interest point and a typhoon is set far from 1500 km at which the wave speed is very low and has little effect on the wave heights.

An effective NN model must pass both model calibration and model verification. The model calibration is a validation of model simulation capacity for the learning data.

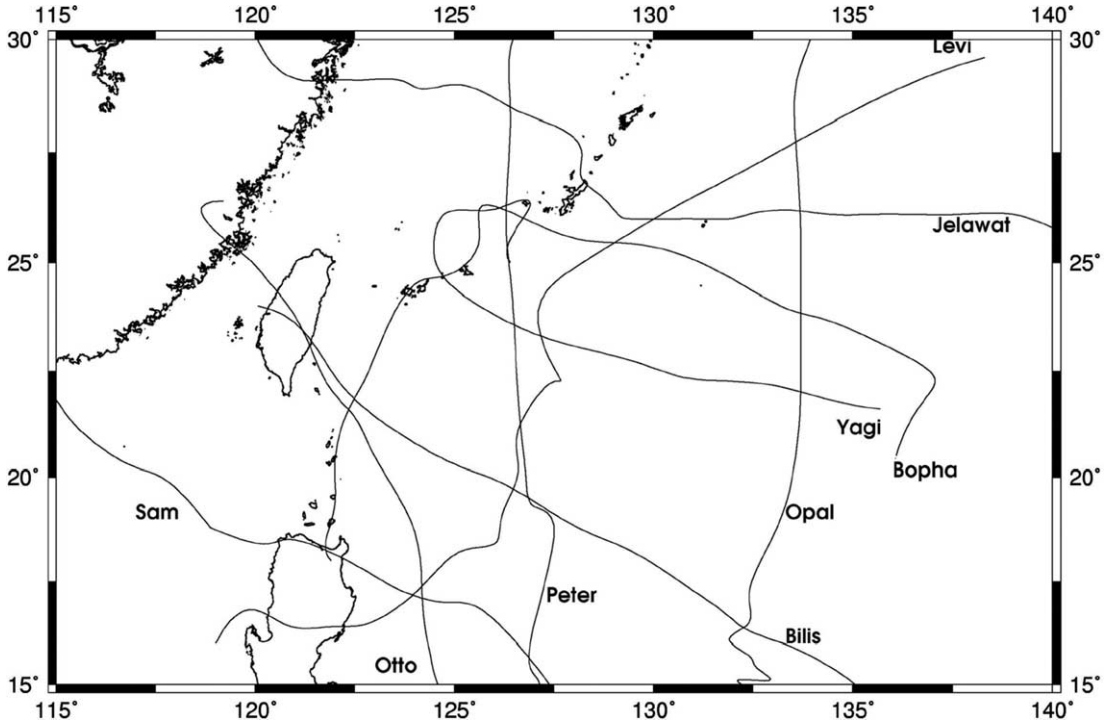

Fig. 10. Paths of nine typhoons considered in the learning stage.

The verification examines the model obtained also holding a high capacity of simulating the data that are not used in the leaning data.

The root mean square (RMS) is commonly used to illustrate the simulation performance of each model. The root mean square is defined as

$$\mathrm{RMS} = \sqrt{\frac{1}{m}\sum_{i=1}^{m}[H_{sm}(t_i) - H_{sp}(t_i)]^2} \tag{12}$$

where $H_{sm}(t_i)$ and $H_{sp}(t_i)$ represent the observed and calculated wave height at time t_i, respectively, and m is the total number of data. Small RMS reveals that a model is very valid for simulating wave heights. The maximum wave height and the times at which it occurs are important in practical engineering. Two alternative indices of simulation performance are defined: they are the difference between the peak observed wave height and the corresponding calculated value, ΔH_{sp}, and time lag between the corresponding times, Δt_p:

$$\Delta H_{sp} = H_{sp,p} - H_{sp,m} \tag{13}$$

$$\Delta t_p = t_{p,p} - t_{p,m} \tag{14}$$

where $H_{sp,m}$ and $H_{sp,p}$ are the observed and calculated peak wave heights, respectively; $t_{p,m}$ and $t_{p,p}$ are the times at which these peaks occur. These two indices are further used to evaluate the simulation capability of the NN–MT model.

Table 1 presents RMS, the resulting difference between the peaks and the corresponding time delay in the learning stage and the observed peak wave height. The relative RMS and ΔH_{sp} are defined to be ratios of RMS and ΔH_{sp}–$H_{sp,m}$, and are also list in Table 1. Table 1 indicates that the present NN–MT model has RMS of simulated wave heights within a range of 0.32–0.89 m and the corresponding relative RMS with a range of 0.08–0.27. The predicted wave peaks have various derivation from the observed ones by 0.1–1.0 m, and the corresponding relative difference of peak wave heights is within a range of 0.05–0.19. A large difference occurs when the observed peak is higher, e.g. Otto (1998) and Bilis (2000). These two typhoons are the first two largest RMS among the examined typhoons.

Time delay of the predicted peaks from the observed ones varies from 0 to 5 h. When the peak is large, the model can accurately give the occurrence time of the peak than when the peak is low. The observed wave heights commonly fluctuate in time due to the time variation of typhoon wind speeds. When typhoon path moves far away from the Hua-Lien harbor the wave heights are generally small. Thus, fixing the occurrence time of the peaks when wave heights have a high peak and sharp variation is easier than when wave heights have a low peak and flat variation. Larger time delay predicted occurs for a far typhoon path, e.g. Levi (1997). Tropical storm Bopha (2000) formed at the far east of Taiwan was first advanced in a westerly direction and had a dramatic southward turn. Bopha continued moving south along Taiwan's east coast and as the storm disappeared into the Bashi Channel, south of Taiwan. Bopha's unusual north-to-south path has not been seen in Taiwan for more than four decades. The unusual path caused the model to have poor simulation on the occurrence time of wave peak.

4.2. Model verification

Here, three typhoons are selected, Fred (1994), Kent (1995), and Haiyan (2001), for simulating wave heights at the Hua-Lien harbor, and apply Maggie (1999) typhoon to the Su-Au harbor, whose paths are presented in Fig. 11. Three NN models are used to compare the prediction capability of wave heights.

One is the previous NN2 models of Chang et al. [4]. The second model, NN3, is set up to add θ_2 input parameter to NN2 model. However, the transfer functions in NN3 model are all expected in the Matlab and differ from multi-trend transfer functions used in the proposed NN–MT model. The transfer functions for each input parameter in these three models and their model constructions are arranged in Table 2.

Table 3 compares RMS, ΔH_{sp} and Δt_p obtained using three modes in the verification stage. The value in the bracket of each column in Table 3 indicates the relative value that is defined as the ratio of RMS, ΔH_{sp} and Δt_p–$\Delta H_{sp,m}$. The mean of relative RMS of four typhoon waves obtained by each model is 0.116, 0.150 and 0.119, respectively. The corresponding standard deviation is 0.032, 0.028 and 0.039, respectively. Comparing RMS

Table 1
RMS, ΔH_{sp}, Δt_p and $H_{sp,m}$ of the wave heights computed by the NN–MT model in the learning stage

Typhoon	RMS (m)	RMS/$H_{sp,m}$	ΔH_{sp} (m)	$\Delta H_{sp}/H_{sp,m}$	ΔH_{sp} (h)	$H_{sp,m}$ (m)
Levi (1997)	0.52	0.27	0.37	0.19	5	1.92
Opal (1997)	0.25	0.13	0.02	0.01	0	1.97
Peter(1997)	0.32	0.10	−0.36	0.11	0	3.19
Otto (1998)	0.89	0.11	−1.00	0.12	0	8.03
Sam (1999)	0.44	0.11	0.37	0.10	2	3.89
Jelawat(2000)	0.51	0.26	−0.10	0.05	−2	1.97
Bilis (2000)	0.65	0.08	−0.52	0.06	−3	8.39
Bopha (2000)	0.45	0.16	0.22	0.08	5	2.78
Yagi (2000)	0.63	0.22	0.24	0.08	4	2.89

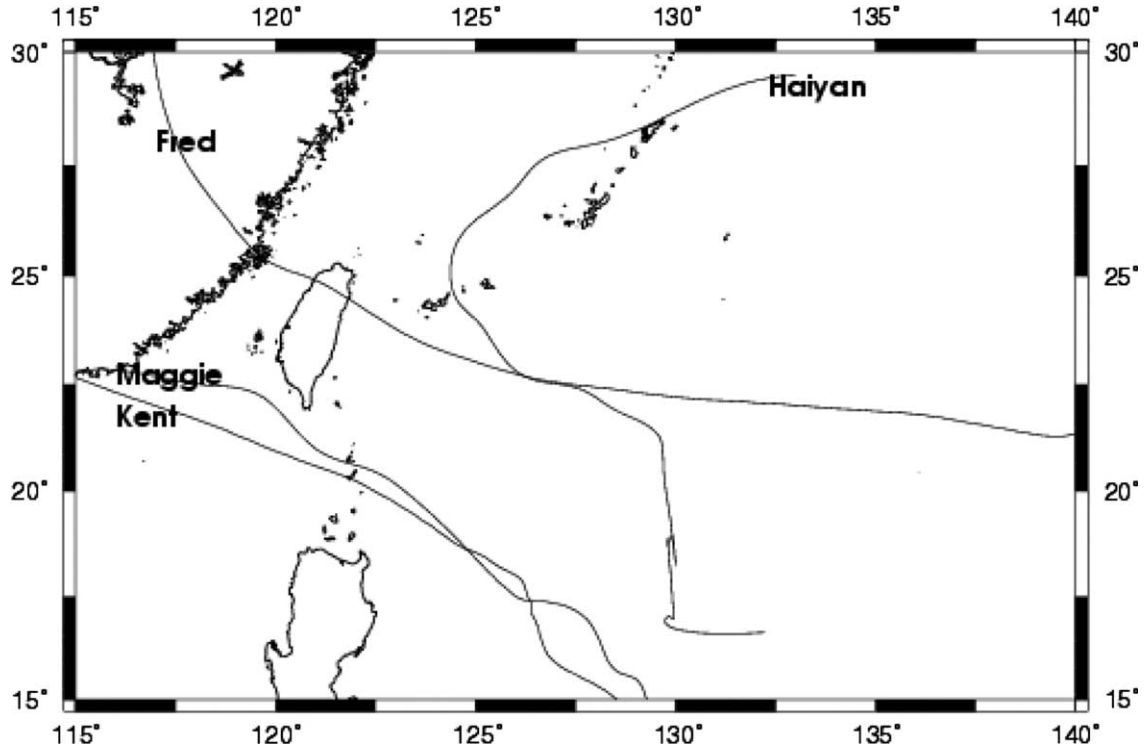

Fig. 11. Paths of four typhoons used in the verification stage.

and the mean of relative RMS clearly reveals that the NN2 and NN–MT models yield smaller RMS than does the NN3 model. The mean of relative ΔH_{sp} of four typhoon waves obtained by each model is 0.132, 0.136, and 0.120, respectively. The corresponding standard deviation is 0.086, 0.080, and 0.041, respectively. Smaller mean of relative ΔH_{sp} and standard deviation obtained by the NN–MT model than those obtained by the NN2 and NN3 models shows that the NN–MT model more accurately calculates the wave peaks than the NN2 and NN3 model do. The NN2 model and the proposed NN–MT model more accurately predict the occurrence time of peak wave height by an error

Table 2
The transfer functions for each input parameter in NN2, NN3 and NN–MT models and their model constructions

Model	Transfer function for each input parameter				Model construction
	$\bar{V}_{10}$	$\bar{r}$	$\bar{\theta}_1$	$\bar{\theta}_2$	
NN2	Satlin	Radial basis	Satlin	Null	39-80-40-2
NN3	Satlin	Radial basis	Satlin	Satlin	36-80-40-1
NN–MT	$f_{\bar{V}_{10}}$	$f\bar{r}$	$f_{\bar{\theta}_1}$	$f_{\bar{\theta}_{21}} f_{\bar{\theta}_{22}} f_{\bar{\theta}_{23}} f_{\bar{\theta}_{24}}$	49-80-40-1

Note: Radial-basis $= e^{-r^{-2}}$; Satlin$(n)=0$, if $n \le 0$, n; if $0 \le n \le 1$, 1; if $1 \le n$, 1.

Table 3
Comparisons of RMS, ΔH_{sp} and Δt_p obtained using NN2 and NN3 models with those obtained using the present NN–MT model in the verification stage

	Model	Fred	Kent	Haiyan	Maggie[a]
RMS (m)	NN2	1.01 (0.150)	0.76 (0.121)	0.29 (0.065)	0.78 (0.131)
	NN3	1.24 (0.184)	0.88 (0.140)	0.49 (0.109)	0.99 (0.166)
	NN–MT	1.18 (0.175)	0.60 (0.095)	0.33 (0.073)	0.80 (0.134)
ΔH_{sp} (m)	NN2	−1.47 (0.218)	−0.47 (0.075)	−0.96 (0.214)	0.13 (0.022)
	NN3	−1.00 (0.148)	−1.09 (0.173)	−0.98 (0.218)	0.03 (0.005)
	NN–MT	0.45 (0.067)	−1.14 (0.181)	−0.55 (0.122)	−0.65 (0.109)
Δt_p (h)	NN2	3	−2	1	−1
	NN3	2	0	−7	−1
	NN–MT	1	−1	3	2
$H_{sp,m}$ (m)		6.75	6.29	4.49	5.96

[a] Denotes the simulation for the Su-Ao harbor.

of less than 3 h than the NN3 model does. The proposed multi-trend transfer functions are more fitting to the measured data than the traditional transfer functions so that the proposed NN–MT model can be validly applicable for common cases. The NN2 and NN3 models are good at calculating the typhoon waves when the typhoon's path is similar to one of those used in the learning stage. However, the NN2 and NN3 models become worse to calculate the typhoon waves when the typhoon's path is far from any one of those used in the learning stage.

The transfer function for $\bar{\theta}_2$ in four quarters model prevents the proposed NN–MT model from the abnormal $\bar{\theta}_2$ data input and effectively describes how $\bar{\theta}_2$ affects waves. Two following figures compare in detail the wave height simulation in time series for each typhoon using three NN models.

After typhoon Fred (1995) was formed and then traveled for 300 h, it passed through the north of the island and had a regular path as shown in Fig. 11. Fig. 12 plots the wave heights computed by three models. The time counts from the formation of the typhoon. When typhoon Fred arrived in Taiwan, Hua-Lien harbor was under the left half of the typhoon. The wave heights computed by both models for the period in which wind waves grew exceeded the observed heights by around 1 m. However, when typhoon Fred reached Taiwan, the peak computed wave height was much lower than the observed peak height by 2.66 m for model NN3 and 1.0 m for NN2 model; however, NN–MT model gave a high prediction only by 0.45 m. NN3 simulated a wave peak time of 2 h after the actual peak was observed, and NN2 simulated a peak 3 h too late. NN–MT model simulated 1 h time delay after the actual peak. When typhoon Fred passed Taiwan, observed wave heights decayed very fast due to very high mountains in central Taiwan and the computed wave heights decayed slowly because of higher wind speeds input in the model than the real values. The land effects on the wind whenever a typhoon passes through Taiwan are complicated and will be studied in the future to modify the model.

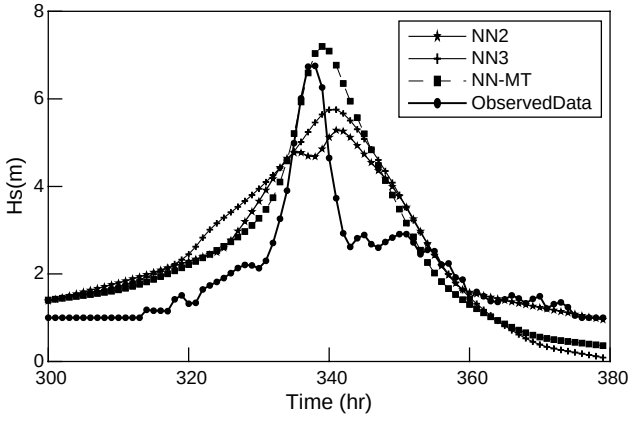

Fig. 12. Wave heights observed at Hua-Lien harbor and computed by three NN models for typhoon Fred (1994).

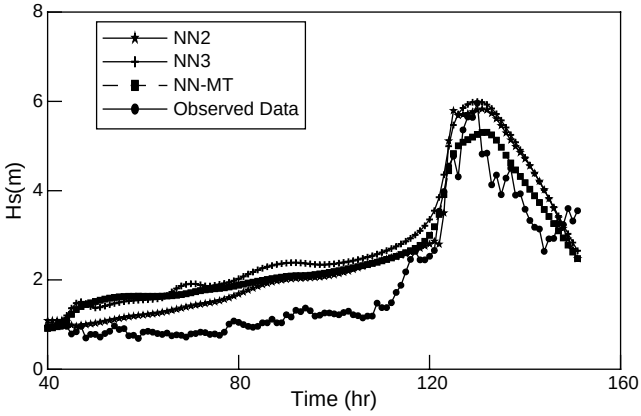

Fig. 13. Wave heights observed at Su-Ao harbor and computed by three NN models for typhoon Maggie (1999).

Only one wave record of typhoon Maggie (1999) at the Su-Ao harbor was available for extending the proposed models to the Su-Au harbor. As indicated in Fig. 11, typhoon Maggie originally formed over the waters to the southeast of Taiwan and moved west by northwest, passing through the Bashi Channel, finally reaching southeast China. Fig. 13 shows the computed and observed wave heights during typhoon Maggie. While Maggie was far from the Su-Ao harbor, the computed wind speeds exceeded the real wind speeds because the Su-Ao harbor was then located in the right semi-circle of typhoon Maggie. The computed wave heights are approximately 1 m lower than the observed heights. The NN2 model simulates the wave heights much better than the NN3 an NN–MT models do when typhoon Maggie roughly reached Taiwan. NN2 yielded a reasonably accurate peak with a 1-h delay. Through the examination on the wave heights predicted for the typhoon Maggie (1999) at the Su-Ao harbor, the proposed NN–MT model is proven to be applicable for calculating the typhoon waves at an interest point along the Taiwan eastern coast.

Both cases of only one typhoon occurring at a time and tropical depressions are excluded in the typhoon data used for the learning stage in the proposed model. Thus, the proposed models cannot be applied to predicting waves caused by monsoons. From the discussion above the present results indicate that the present model is limit to the conditions that the typhoons are affected by high mountains or the roughness of the land and they move from the east towards the west.

5. Conclusions

Chang et al. [4] proposed two applicable NN models to support rapid computation to determine the relationship between typhoon winds and waves. When the number of input data is small or the data are abnormally distributed, an NN model is hard to set up for accurate simulating wave

heights. An appropriate transfer function that can certify the model for most cases and prevent from the disadvantage of over-learning problems is required for a good NN model. The present work first considered multi-trend simulating transfer functions in NN model to more stably and accurately calculate wave heights than the former two models. The proposed NN–MT model can be applicable for the path of an examined typhoon that may be not similar to some paths of the typhoons chosen in the learning stage.

Four essential factors influencing typhoon waves are discussed and expressed by suitable trend functions. They are the local wind speed at 10 m high, distance between the interesting point and typhoon's center, the azimuth angle and the position angle in a moving typhoon. The last factor is to express the difference that wind speed in the right semi-circle is larger than that in the left semi-circle. Four equal quarters in a circle are separated to have the proposed transfer Gussian functions that can provide the model sensible description of wind speed distribution when wind speed data are less. The present NN–MT model can precisely simulate the peak of typhoon waves by an error of less than 1.2 m in height and by a shift of 3 h in occurrence time.

The NN models are extended to calculate wave heights at the Su-Ao harbor that is next to the Hua-Lien harbor. The proposed model also accurately predicts wave heights. However, the NN models fail to simulate the decay of waves due to land with high mountains. The land effect should be more closely examined in the future.

References

[1] Booij N, Holthuijsen LH, Ris RC. The SWAN wave model for shallow water. Proc 24th Conf Coastal Eng 1996;1:668–76.
[2] Bretschneider CL, Tamaye EE. Hurricane wind and wave forecasting techniques. Proc 15th Conf Coastal Eng 1976;1:202–37.
[3] Chalikov DV, Makin VK. Models of wave boundary layer. Bound-Lay Meteorol 1991;56:83–99.
[4] Chang HK, Chien WA, Ho LS. Neural network models of typhoon waves in the waters east of Taiwan. Submitted for publication.
[5] Chen YH, Wang H. Numerical model for non-stationary shallow water wave spectral transformation. J Geophys Res 1983;88:9851–63.
[6] Deo MC, Naidu CS. Real time wave forecasting using neural networks. Ocean Eng 1998;26:191–303.
[7] Deo MC, Jha A, Chaphekar AS, Ravikant K. Neural networks for wave forecasting. Ocean Eng 2001;28:889–98.
[8] Eberhart RC, Dobbins RW. Neural network PC tools—A practical guide. San Diego: Academic Press, Ins.; 1990 p 10–250.
[9] Hajime M, Sakamoto M, Sakai T. Neural network for stability analysis of rubble-mound breakwaters. J Waterw Port Coast Ocean Eng 1995;97:139–54.
[10] Harper BA, Holland GJ. An updated parametric model of the tropical cyclone. Proc 23rd Conf Hurricane Tropical Meteorol 1999;893–6.
[11] Hiraoka T, Maeda H, Ikoma N. Two-stage prediction method of typhoon position by fuzzy modeling-fusion of outline prediction and detailed prediction systems. Proc IEEE SMC '99 Conf Man Cybernetics 1999;6:581–5.
[12] Holland GJ. An analytical model of the wind and pressure profiles in hurricanes. Mon Weather Rev 1980;108:1212–8.
[13] Jelesnianski CP. Numerical computations of storm surges without bottom stress. Mon Weather Rev 1966;94(6):379–94.
[14] Johnson GP, Lin FC. Hurricane tracking via backpropagation neural network. Proc IEEE Conf Neural Networks 1996;2:1103–6.
[15] Kinsman B. Wind waves, their generation and propagation on the ocean surface. Englewood Cliffs, NJ: Prentice-Hall, Inc.; 1965.
[16] Komen GJ, Cavaleri L, Donelan M, Hasselmann K, Hasselmann S. Janssen PAEM. Dynamics and modeling of ocean waves. Cambridge: Cambridge University Press; 1994 p 532.
[17] Krasitskii VP. On the generation of wind waves on the initial stage. Izv Akad Nauk SSSR Ser Fiz Atm i Okeana 1980;10:72–82.
[18] Lee RST, Liu JNK. An elastic graph dynamic link model for tropical cyclone pattern recognition. Proc 6th Conf Neural Inf 1999;1:177–82.
[19] Lippman RP. An introduction to computing with neural nets. IEEE ASSP Magazine 1987;4:14–24.
[20] Niwa Y, Hibiya T. Nonlinear processes of energy transfer from traveling hurricanes to the deep ocean internal wave field. Oceanograph Lit Rev 1998;45:39.
[21] Riley DS, Donelan MA, Hui WH. An extended Miles' theory for wave generation by wind. Bound-Lay Meteorol 1982;22:209–25.
[22] SWAMP Group (24 Authors). Ocean wave modeling. New York: Plenum Press; 1985. P. 256.
[23] Tsai CP, Lee TL. Back-propagation neural network I tidal-level forecasting. J Waterw Port Coast Ocean Eng 1991;12(4):195–202.
[24] Tolman HL. User manual and system documentation of WAVE-WATCH-3, 1997; version 1.15, NOAA/NWS/NCEP/OMB Technical Note 151, p 97.
[25] WAMDI group the WAM model. A third generation ocean wave prediction model. J Phys Oceanogr 1988;18:1775–7810.
[26] Young IR. A parametric hurricane wave prediction mode. J Waterway Port Coast Ocean Eng 1988;114:352–637.